Journal of Statistical Physics, Vol. 114, Nos. 1/2, January 2004 (© 2004)

Dynamical Windings of Random Walks and Exclusion Models. Part I: Thermodynamic Limit in $\mathbb{Z}^2$

Guy Fayolle[1, 2] **and Cyril Furtlehner**[1, 2]

Received November 28, 2002; accepted June 18, 2003

We consider a system consisting of a planar random walk on a square lattice, subjected to stochastic elementary local deformations. Both numerical and theoretical results are reported. Depending on the deformation transition rates, and specifically on a parameter η which breaks the symmetry between the left and right orientation, the winding distribution of the walk is modified, and the system can be in three different phases: folded, stretched and glassy. An explicit mapping is found, leading to consider the system as a coupling of two exclusion processes: particles of the first one move in a landscape defined by particles of the second one, and vice-versa. This can be viewed as an inhomogeneous exclusion process. For all closed or periodic initial sample paths, a convenient scaling permits to show a convergence in law (or almost surely on a modified probability space) to a continuous curve, the equation of which is given by a system of two non linear stochastic differential equations. The deterministic part of this system is explicitly analyzed via elliptic functions. In a similar way, by using a formal fluid limit approach, the dynamics of the system is shown to be equivalent to a system of two coupled Burgers equations.

KEY WORDS: Random walks; winding; exclusion process; phase transition; Burgers equation.

1. INTRODUCTION

Random walks are fundamental objects arising in probability. Also they are of primary importance in various fields of physics, especially with regard to polymers[11, 8] and biology. For instance, planar random walks can be used as a representation of DNA coding, since the sequence of the

[1] INRIA-Domaine de Voluceau, Rocquencourt BP 105-78153 Le Chesnay Cedex, France.
[2] E-mail: Guy.Fayolle@inria.fr; Cyril.Furtlehner@inria.fr

0022-4715/04/0100-0229/0 © 2004 Plenum Publishing Corporation

four different kinds of codons (A,G) for purines and (T,C) for pyrimidines can be considered as a random walk on a square lattice: as a rule, (G,C) code the upward and downward jumps, whereas (A,T) code the left and right steps.[1,4] It seems therefore interesting to consider random geometrical objects as complex systems, and to submit them to some dynamical principles, the goal being to develop methods and tools which hopefully might be used to tackle more realistic models.

In this context we will analyze the evolution of an arbitrary sample path $\mathbf{C}_N$ of length N, generated by a *simple* random walk in the square lattice $\mathbf{Z}^2$, and subject to local transformations. This stochastic object has a rich structure, plays an important role in probability theory and lends itself to sufficiently wide but non trivial results.

At time $t = 0$, $\mathbf{C}_N$ is given, and we assume it has been uniformly generated. This means precisely that each successive jump (up, down, left, and right) building $\mathbf{C}_N$ is selected with the same probability $1/4$. Eventually $\mathbf{C}_N$ can be constrained to be closed or to have fixed extremities. Once the initial configuration is defined, the system evolves according to the four local pattern transformations depicted in Fig. 1. Only a single point of the walk can be moved at a time, with the constraint that no link be broken (i.e., the walk remains always connected).

Geometrically, these patterns can be expressed as

$$\begin{cases} \text{left bend } M1, \text{ right bend } M3, \\ \text{vertical or horizontal fold } M2, \\ \text{straight } (\rightarrow \rightarrow)\ M4, \end{cases}$$

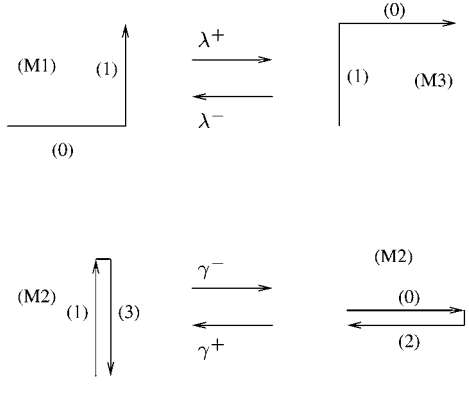

Fig. 1. Pattern transition rates.

and the following local distortions can occur:

$$\begin{cases} M1 \to M3, \text{ with rate } \lambda^+, \\ M3 \to M1, \text{ with rate } \lambda^-, \\ \text{rotation of } M2 \text{ of angle } \pm \frac{\pi}{2}, \text{ with rate } \gamma^{\pm}. \end{cases}$$

Hence we have defined a global Markovian continuous time evolution of the system, with exponentially distributed jump times, the state space of the underlying Markov chain being the set of 4^N sample paths (or curves) $\mathbf{C}_N$ introduced above.

This model is somehow a kind of discrete analogue of the Rouse chain,[20] which is a popular model for polymer dynamics. There, each point of the chain is harmonically bound to its nearest neighbor, and move randomly in space. Some interesting statements can be made concerning the winding properties of such chains in 2d.[2] In this respect, from a probabilistic point of view, we keep in mind that winding variables are for Brownian curves, and they give rise to striking limit laws under convenient scalings (see, e.g., refs. 21, 18, and 19).

The paper is organized as follows. Section 2 presents the basic numerical and qualitative results, which rely on *ad hoc* discrete event simulation experiments together with a convenient graphical interface. In Section 3, we propose a mapping of this model onto another one, which consists of two coupled exclusion processes. The main quantitative results are given in Section 4: scaling parameter, phase transition and critical value, fluctuation analysis via theorems of central limit type.

2. NUMERICAL EXPERIMENTS

2.1. Observations

We shall begin our study with several basic numerical observations. The model is purely stochastic and hence well-suited for Monte-Carlo simulations. These have been performed with the help of a graphical interface, which facilitates the exploration of the relevant parameter range, together with the display of the main regimes and phases of the system.

Several parameters have to be tuned: the number of steps N; the relative position of the extremities of the walk (D_x, D_y); the boundary conditions, which either can be defined to let the end points move independently, or can be fixed or tied up by some periodic boundary conditions; finally, the time constants associated with the elementary transformations, τ_1 with γ, τ_2 and τ_3 with λ^+ and λ^-. Any walk fulfilling these conditions is randomly generated at time $t = 0$ and then evolves stochastically, with a movement depending on the rates and boundary conditions given above.

After each new event, time is incremented by an amount inversely proportional to the number of all possible moves weighted by their respective rates.

Interesting things happen when we break the chiral symmetry by imposing a *detuning* between λ^+ and λ^-, in a proportion of order

$$\eta = N \frac{\lambda^+ - \lambda^-}{\lambda^+ + \lambda^-}. \tag{2.1}$$

For closed walks, four different situations can roughly be observed (see Fig. 2).

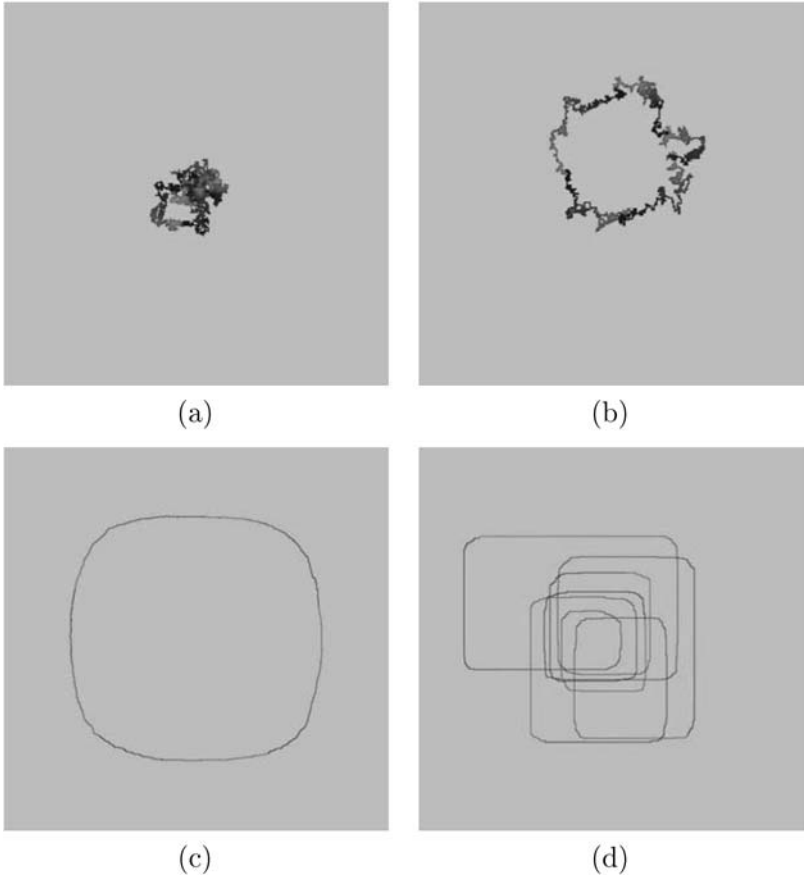

Fig. 2. Picture of a random walk of $N = 5000$ steps, showing the phases of the system for several values of η. Each dark line segment represents 1000 steps. (a) $\eta = 0$ (the basic scale). (b) $\eta = 5$ (scale $= 1$). (c) $\eta = 12.5$ (scale $= 1/6$). (d) $\eta = 250$ (scale $= 1/2$).

(a) $\eta \lesssim 1$. The initial configuration belongs to the equilibrium set of typical configurations, only fluctuations are altered by the finite value of η.

(b) $1 \lesssim \eta \lesssim 6$. The system reaches an equilibrium which still corresponds to a random walk, the fractal dimension remaining equal to two, but a macroscopic circular drift is observed, yielding a sort of smoking ring.

(c) $6 \lesssim \eta \lesssim 50$. The smoking ring gets stretched, and the elementary links becomes aligned over long distance. Fractal dimension shrinks to one, with the apparition of a long range order. Rotational invariance is broken.

(d) $\eta \gtrsim 50$. The system is not able to reach its equilibrium. This typical configuration (out of equilibrium) exhibits an intricate hierarchical structure of bubbles. Smaller bubbles get evaporated into bigger bubbles. Time constants associated to these mechanisms grow exponentially with the size of the bubbles. Therefore, the final configuration corresponding to one bubble is never reached in the thermodynamic limit. We will refer to this non-equilibrium phase as a *glassy* phase.

2.2. Brownian Windings

Some macroscopic random variables of interest can be constructed in order to be able to follow numerically the evolution of the system. First of all the total number of patterns $M1$, $M2$, $M3$, $M4$ is a set a variables which can be used to distinguish between a folded and a stretched phase of the system. All these number are expected to be fairly distributed in the folded phase although in the stretched phase we expect the pattern $M4$ to be in majority. In order to express mathematically the curling of the system, we consider variables related to the winding properties of planar Brownian curves, which are defined as follows: with each point in the plane is associated its *winding angle* θ, scanned by the random walker around this point. A limit law for this variable has been derived by Spitzer for Brownian curves. Actually, assuming the length of the curve is set to $2\ell = Na^2$ when $N \to \infty$ and $a \to 0$ in the Brownian limit, the winding angle $\theta(\ell)$ of an arbitrary point has the asymptotic probability[21]

$$\lim_{\ell \to \infty} P\left(\theta(\ell) = \frac{\alpha \log \ell}{2}\right) = \frac{1}{\pi} \frac{1}{1+\alpha^2}.$$

For a closed walk, the value taken by θ are limited to $2n\pi$, where $n \in \mathbb{Z}$ represents the *winding number* associated with the point under consideration.

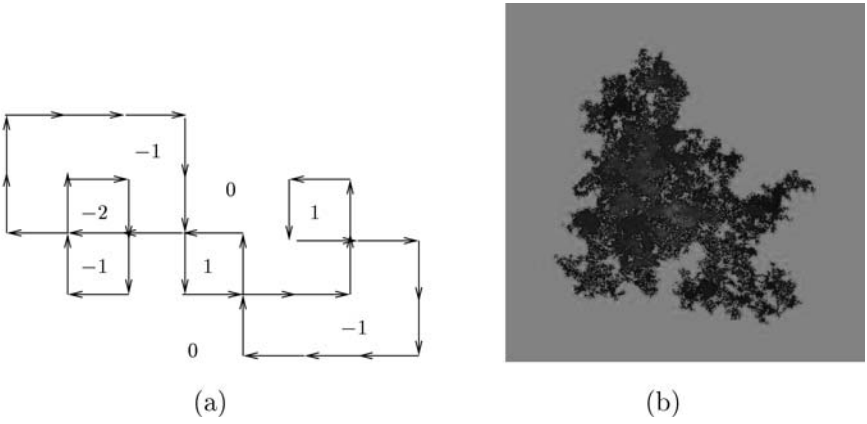

Fig. 3. Winding sectors defined for a closed random walk (a). Intensity gradient representing sectors for a walk of $N = 10^6$ steps: in dark gray and black, respectively, positive and negative winding sectors; in light gray, the null sector (b).

For each n, the set of points with the same winding number n form a *winding sector*, whose arithmetic area is a random variable denoted by $S_n(\ell)$.

Under the above mentioned Brownian limit for closed curves of length ℓ, we have[6]

$$\mathbb{E}[S_n(\ell)] = \frac{\ell}{2\pi n^2}.$$

In a similar way, the total *algebraic area* enclosed by the Brownian curve is defined as

$$A(\ell) = \sum_{n \in \mathbb{Z}} n S_n(\ell),$$

and its distribution is given by Lévy's law[18]

$$\lim_{\ell \to \infty} P(A(\ell) = 2s\ell) = \frac{\pi}{2\cosh^2(\pi s)}.$$

The variable $S_n(\ell)$ is indeed enough for a complete characterization of the phases of the system.

2.3. Slow Dynamics

The study of winding sectors and of associated variables is especially well adapted to describe the evolution of the system, since the presence of

curls has a direct impact on the S_n distribution. A small but finite value of $\eta \lesssim 1$ will show itself by the existence of a shift in the distribution of S_n together with an unbalancing between positive and negative winding sectors. When $1 \lesssim \eta \lesssim 6$, the distribution of S_n condenses into either S_1 or S_{-1}. However, the behavior of S_1 or S_{-1} with regard to scaling factor does not change, and these variables still scale like N. The system reaches its stationary state after a transient regime characterized by a single time constant (Fig. 4a). For $6 \lesssim \eta \lesssim 50$ the system get stretched, an unfolding transition occurs. S_1 or S_{-1} scale now like N^2, and the fact that the walk is tight get reflected in the distribution of the motifs M_1, M_2, M_3, M_4. When $\eta \gtrsim 50$ we obtained a glassy phase. This is related to the apparition of a hierarchy distribution of meta-stable configurations. The system evolves slowly to the rate of bubbles evaporations, small bubbles collapses and produce bubbles of bigger size. As a consequence, the transitory regime is completely different. For small size systems (see Fig. 4b), it is observed that

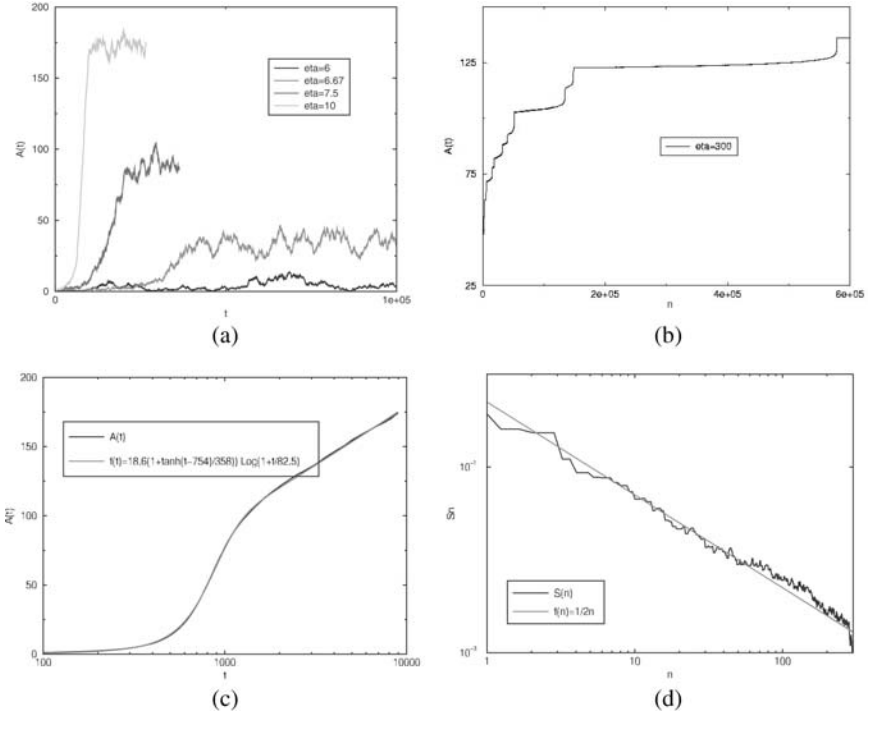

Fig. 4. Evolution of the total algebraic area (a, b, c). First transition with condensation in the first winding sector (a) $N = 1000$ steps. Unfolding transition with metastable states for $N = 2000$ steps (b). Curves (c) and (d), drawn in a logarithmic scale for $N = 10^6$, represent respectively the slow dynamics and the distribution of the S_n's.

the total algebraic area increases by successive steps. These steps correspond to intermediate metastable states, consisting of bubbles of increasing size. The associated time constants behave roughly exponentially with the size of these bubbles. When $N \to \infty$ (see Fig. 4c), a continuous spectrum of time constants is obtained and the convolution of these dynamical effect corresponding to different scale end up in a slow dynamical grows. The total algebraic area increases logarithmically with time. We observe also (see Fig. 4d) that the distribution of S_n seems to have a limit characterized by the absence of negative (or positive) sectors, i.e., strictly zero for negative (or positive) index n, together with a scaling exponent around 1. Indeed this sequence of distributions seems to behave like n^{-1}, instead of n^{-2} for $\eta = 0$. Also the glassy transition is clearly of first order, with coexistence of a liquid phase (part of the walk which remains folded and disordered) and a solid glassy phase. The parameters corresponding to temperature and magnetization can be defined by analogy with standard

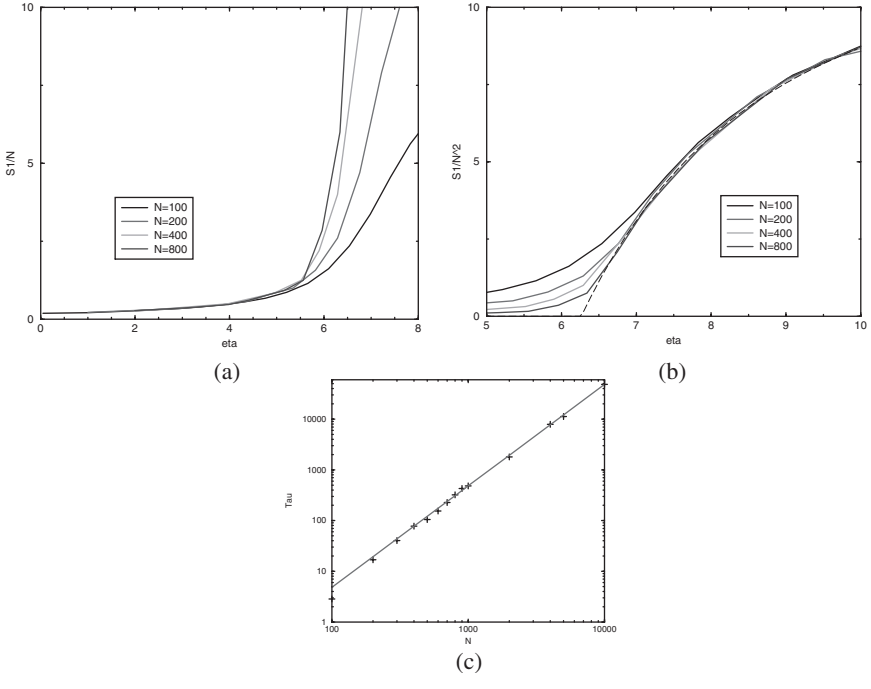

Fig. 5. The limit arithmetic area of the first winding sector when η varies, rescaled by N (a) and by N^2 (b). The dashed line in (b) is computed from part 4.2 giving the critical value $\eta_c = 2\pi$ separating the folded phases from stretched one. Scaling with N of time-constants for the transient regime (c) for $\eta = 10$; the fit gives a value 2.01 for the exponent.

spin glasses. They can be tuned independently, as we shall see later on, by letting vary η (which is roughly equivalent to the external magnetic field) and γ (pertaining in some sense to the temperature).

3. MAPPING ONTO COUPLED EXCLUSION PROCESSES

3.1. Sequence Coding

The entire walk can be encoded in a sequence (α_i) of four integers $(0, 1, 2, 3)$, corresponding to the orientation of the each link $i \in \{1 \ldots N\}$ in units of $\frac{\pi}{4}$, connecting two successive points.

The local deformations are expressed as local exchanges or reactions between neighbouring sites. The set of reactions is described as follows:

$$01 \underset{\lambda^+}{\overset{\lambda^-}{\leftrightarrows}} 10, \qquad 12 \underset{\lambda^+}{\overset{\lambda^-}{\leftrightarrows}} 21, \qquad 23 \underset{\lambda^+}{\overset{\lambda^-}{\leftrightarrows}} 32, \qquad 30 \underset{\lambda^+}{\overset{\lambda^-}{\leftrightarrows}} 03,$$

$$02 \underset{\gamma^+}{\overset{\gamma^-}{\leftrightarrows}} 13, \qquad 13 \underset{\gamma^+}{\overset{\gamma^-}{\leftrightarrows}} 20, \qquad 20 \underset{\gamma^+}{\overset{\gamma^-}{\leftrightarrows}} 31, \qquad 31 \underset{\gamma^+}{\overset{\gamma^-}{\leftrightarrows}} 02.$$

When looking carefully at the transitions, as skeched in Fig. 6, we observe that two independant processes are at work. Indeed, mutations operate either vertically or horizontally, and with opposite directions between both modified links. This suggests to recode each link j, $j = 1, \ldots, N$ by means of two binary components $s_j^a \in \{0, 1\}$ and $s_j^b \in \{0, 1\}$, where s_j^a represents the column index and s_j^b the line index. Thus is established a *bijection* $\alpha_j \to (s_j^a, s_j^b)$ such that

$$\begin{cases} 0 \to (0, 0), \\ 1 \to (1, 0), \\ 2 \to (1, 1), \\ 3 \to (0, 1). \end{cases}$$

In this scheme a transition on an arbitrary link does concern only either of its components. Indeed the infinitesimal generator is the sum of two terms: the first one acts on the sequence $\{s_i^a\}$, with rates conditioned by the sequence $\{s_i^b\}$ and vice-versa. We have thus a Markov process with state space

$$(S^a, S^b) = ((s_1^a, s_1^b), \ldots, (s_N^a, s_N^b)),$$

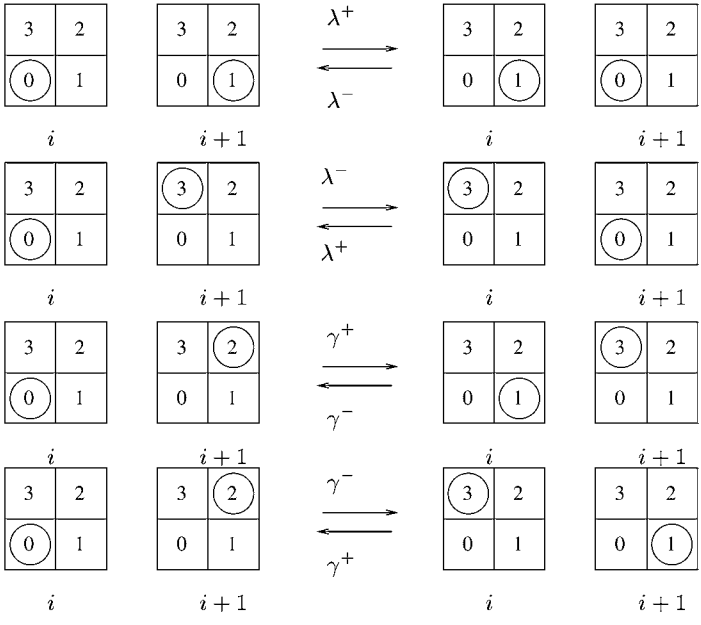

Fig. 6. Horizontal and vertical exchanges corresponding to transitions when link i has the value 0, according to the 4-adic coding. Rules for other transitions follow by rotational symmetry.

which is thus a $2N$-dimensional boolean vector. Then, for an arbitrary function $f\colon (S^a, S^b) \to \mathbb{C}$, the generator decomposes into

$$G = \sum_{i=1}^{N} h_a(i) + h_b(i), \tag{3.1}$$

where the operators h_a, h_b acting on f are defined by

$$\begin{aligned} h_a(i)\, f(S^a, S^b) &\stackrel{\text{def}}{=} \lambda_a^+(i)\, s_i^a \bar{s}_{i+1}^a [f((s_1^a, s_1^b),\ldots,(0, s_i^b),(1, s_{i+1}^b),\ldots,(s_N^a, s_N^b)) - f(S^a, S^b)] \\ &\quad + \lambda_a^-(i) \bar{s}_i^a s_{i+1}^a [f((s_1^a, s_1^b),\ldots,(1, s_i^b),(0, s_{i+1}^b),\ldots,(s_N^a, s_N^b)) - f(S^a, S^b)], \\ h_b(i)\, f(S^a, S^b) &\stackrel{\text{def}}{=} \lambda_b^+(i)\, s_i^b \bar{s}_{i+1}^b [f((s_1^a, s_1^b),\ldots,(s_i^a, 0),(s_{i+1}^a, 1),\ldots,(s_N^a, s_N^b)) - f(S^a, S^b)] \\ &\quad + \lambda_a^-(i) \bar{s}_i^b s_{i+1}^b [f((s_1^a, s_1^b),\ldots,(s_i^a, 1),(s_{i+1}^a, 0),\ldots,(s_N^a, s_N^b)) - f(S^a, S^b)], \end{aligned}$$

using the boolean notation $\bar{s} = 1 - s$. Transition rates can be computed by inspecting the different cases, which yields the following expressions.

$$\begin{cases} \lambda_a^{\pm}(i) = \bar{s}_i^b \bar{s}_{i+1}^b \lambda^{\mp} + s_i^b s_{i+1}^b \lambda^{\pm} + \bar{s}_i^b s_{i+1}^b \gamma^{\mp} + s_i^b \bar{s}_{i+1}^b \gamma^{\pm}, \\ \lambda_b^{\pm}(i) = \bar{s}_i^a \bar{s}_{i+1}^a \lambda^{\pm} + s_i^a s_{i+1}^a \lambda^{\mp} + \bar{s}_i^a s_{i+1}^a \gamma^{\pm} + s_i^a \bar{s}_{i+1}^a \gamma^{\mp}. \end{cases} \tag{3.2}$$

The generator (3.1) represents two coupled systems of particles moving on a one-dimensional lattice with exclusion (i.e. there is at most one particle of each species per site[17]).

These particles perform random elementary jumps to the left or to the right. Obviously, both systems are interlaced: the jump rates $\lambda_a^{\pm}(i)$ of species (a) at site i are conditioned by the states of particles of species b at sites $i, i+1$, and conversely according to relations (3.2). Here we introduce a notation which will be meaningful in the sequel,

$$\lambda \stackrel{\text{def}}{=} \frac{\lambda^+ + \lambda^-}{2} \quad \text{and} \quad \mu \stackrel{\text{def}}{=} \frac{\lambda^+ - \lambda^-}{2},$$

$$\gamma \stackrel{\text{def}}{=} \frac{\gamma^+ + \gamma^-}{2} \quad \text{and} \quad \delta \stackrel{\text{def}}{=} \frac{\gamma^+ - \gamma^-}{2}, \tag{3.3}$$

In the particular case $\gamma^{\pm} = \lambda^{\pm}$, we get

$$\begin{cases} \lambda_a^{\pm}(i) = \lambda \pm (2s_i^b - 1)\,\mu, \\ \lambda_b^{\pm}(i) = \lambda \mp (2s_i^a - 1)\,\mu. \end{cases} \tag{3.4}$$

In this case, λ represents explicitly the diffusion constant of an isolated particle, with drift μ, the sign of which is determined by s_i^b. A convenient representation of the system is to draw a one-dimensional profile from the sequence $\{s^b\}$ (positive or negative slope depending on whether s^b equals 0 or 1), to sketch the probabilistic inclination to turn left or right, as shown in Figs. 7b and c.

The distribution of particles labeled (a), submitted to the diffusion defined this way, is given by the sequence $\{s^a\}$ (0 or 1 particle depending on the individual site values of s_a). A complementary model is obtained by exchanging the roles of s^a and s^b. In addition, elementary transitions of the system correspond to jumps in the left or right direction of particles (a) and (b). In the complementary formulation, these transitions are materialized through modifications of the profile determined by s^a or s^b (see Fig. 8). Therefore, from this viewpoint, we can formulate the dynamic of subsystem (b) in terms of a KPZ model[13], in which the noise is produced by the distribution of particles (a). With this formulation, the conserved quantities (pointed out earlier) can be obtained in a straight-

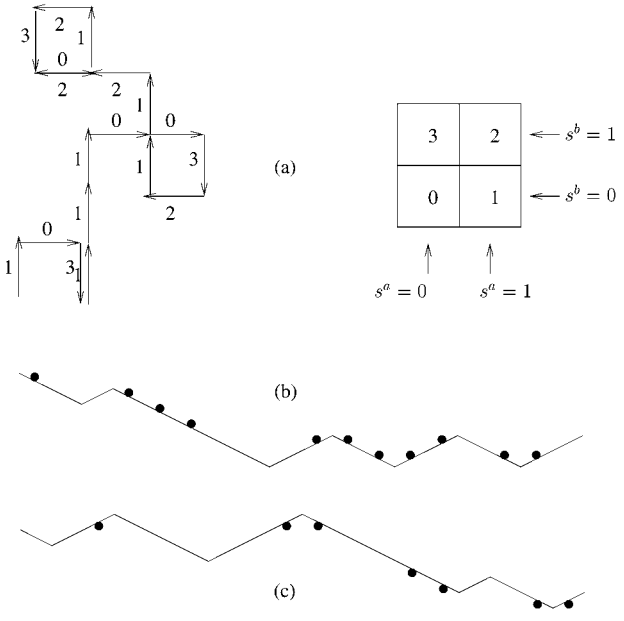

Fig. 7. Correspondence between 4-adic representation of the random walk (a) and one-dimensional models of particle diffusion with exclusion. In (b), the sequence $\{s^a\}$ [resp. $\{s^b\}$] determines the profile of the diffusion [resp. the distribution of particles], drawn for $\gamma^{\pm} = \lambda^{\pm}$; in figure (c) the role of the particles has been exchanged.

forward manner, since they simply express conservation of particles. If boundary conditions are such that particles cannot escape from the system, the population of both species is conserved. This is for example the case when we impose periodic boundary conditions or also when extremities of the chain are fixed.

Suppose we fix the total amount n_a and n_b of particles (a) and (b), this results then on the random walk by the fact that $n_0 + n_3 = n_a$ and $n_0 + n_1 = n_b$ are fixed (n_i is the number of links i). Since $n_0 + n_1 + n_2 + n_3 = N$ it then easy to convince oneself that this is equivalent to fix $n_0 - n_2$ and

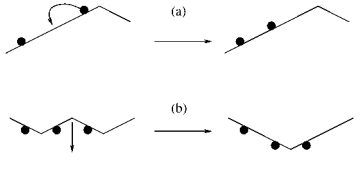

Fig. 8. (a) Elementary transition due to the jump of a type (a) particle, and the part (b) of the figure shows the corresponding deformation of the profile defined by s^a ($\gamma^{\pm} = \lambda^{\pm}$).

$n_1 - n_3$, which is enough to determine the respective positions of the initial and final points of the walk.

In addition, except when $\gamma = 0$, we get an easy way to determine the irreducible classes of the system. In fact, for closed systems with a fixed number of particles, once the population of each species is fixed, just start from the configuration (11..1100..00) for both species where all particles have been disposed to the left. Then, owing to possible consecutive jumps to the right, which for $\gamma \neq 0$ are always authorized, one can reach any arbitrary configuration. This shows that for closed systems irreducible classes are indexed by the number of particles in each species, which corresponds to the separation between extremities of the walk. On the other hand, for open sample paths with free boundary conditions, irreducibility holds as long as particles can both enter and leave the system.

3.2. An Iterative Scheme

An interesting point is the way stable configurations, which are numerically observed, are represented by means of this exclusion process formulation. In agreement with the intuition, Fig. 9 depicts a stable situation where particles are trapped in a well. As this remains true with the complementary representation (see the lower part of Fig. 9b), the following iterative scheme can be used to generate the global invariant measure: let particles (a) evolve assuming the dynamics of particles (b) is frozen; then, once this *conditional* stationary regime is reached, switch to particles (*b*) conditioned by particles (*a*), etc. Translated mathematically, this machinery is tantamount to the following iterative system

$$\begin{cases} X^{n+1} = \lim\limits_{t \to \infty} \mathsf{E}(S^a(t) \mid S^b(t) = Y^n, S^a(0) = X^n), \\ Y^{n+1} = \lim\limits_{t \to \infty} \mathsf{E}(S^b(t) \mid S^a(t) = X^n, S^b(0) = Y^n), \end{cases}$$

which captures the invariant measure of the process as $n \to \infty$. Numerically, the sequences of random variables X^n and Y^n convincingly converge for $\eta < 50$ to the stationary variables $S^a(\infty)$ and $S^b(\infty)$.

Up to an abuse of notation, we shall often identify the random process with any of its sample paths. For instance, we simply write $P(S^a \mid S^b)$ [resp. $P(S^b \mid S^a)$] for the conditional invariant measure of particles (a) [resp. (b)] when the dynamics of particles (b) is frozen. Then the iterative scheme can be reformulated as

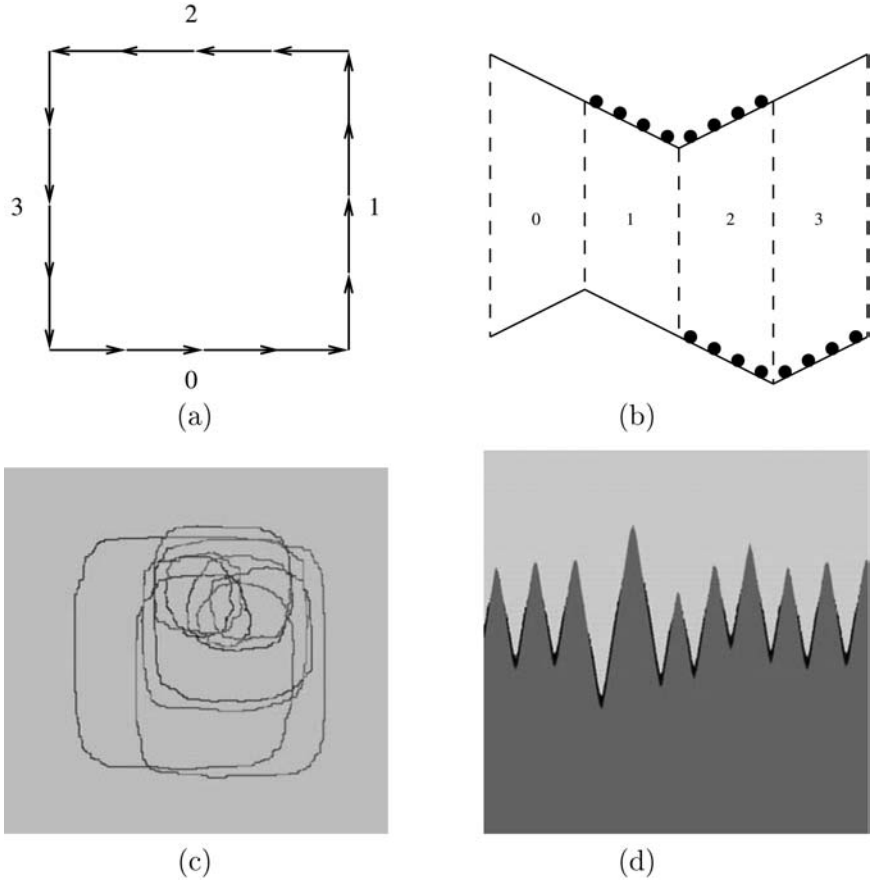

Fig. 9. (a) Stable configuration for closed chains. (b) Corresponding representation in terms of exclusion models. (c) Glassy state with $N = 5000$. (d) Corresponding KPZ landscape with the density of trapped particles appearing in black.

$$Q_{n+1}(S^a) = \sum_{\{S^b\}} P(S^a \mid S^b)\, R_n(S^b),$$

$$R_{n+1}(S^b) = \sum_{\{S^a\}} P(S^b \mid S^a)\, Q_n(S^a),$$

where Q_n [resp. R_n] represents the probability measure of S^a [resp. S^b] after n steps of the algorithm. The invariant joint probability distribution is given by

$$P(S^a, S^b) = P(S^a \mid S^b)\, R(S^b) = P(S^b \mid S^a)\, Q(S^a),$$

where $Q(S^a) = \lim_{n\to\infty} Q_n(S^a)$ and $R(S^b) = \lim_{n\to\infty} R_n(S^b)$.

4. FLUID LIMITS

4.1. Conditional Equilibrium

4.1.1. The Case of a Stretched Walk

Let us have a look to a special case which can be solved exactly. It will provide some hints about scaling of the parameters when $N \to \infty$.

Consider a random walk with fixed extremities, and consisting only of links oriented either to the north or to the east, i.e., $(\alpha_i \in \{0, 1\}, i = 1 \dots N)$. Here folds do not exist (see Fig. 10), so that $s^b = 0$ everywhere and solely transitions $\lambda^{\pm}$ take place. It turns out that the invariant measure has the product-form

$$P(\alpha_1, \dots, \alpha_N) = p_{\alpha_1} p_{\alpha_2} \dots p_{\alpha_N}.$$

Indeed, introducing the occupation rate of particles (a) $q_i = p_1(i) = 1 - p_0(i)$, we have the balance equations

$$\lambda^+(1-q_i)\, q_{i+1} = \lambda^- q_i (1-q_{i+1}). \tag{4.1}$$

Setting

$$r_i \stackrel{\text{def}}{=} \frac{q_i}{1-q_i},$$

we obtain a geometric series

$$r_i = r_0 \left(\frac{\lambda^-}{\lambda^+}\right)^i = r_0 \exp\left[i \log \frac{1-\eta/N}{1+\eta/N} \right]. \tag{4.2}$$

In (4.2), the ratio

$$\frac{\eta}{N} = \frac{\lambda^+ - \lambda^-}{\lambda^+ + \lambda^-} = \frac{\mu}{\lambda},$$

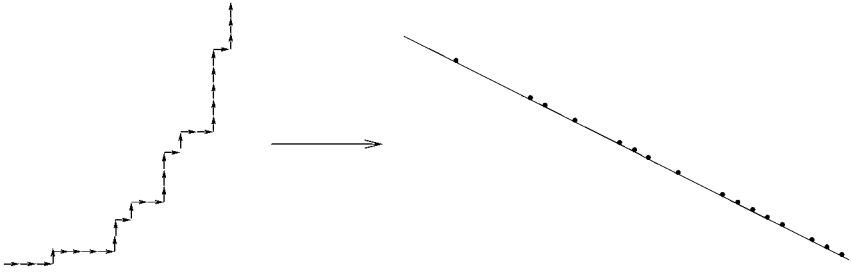

Fig. 10. Stretched random walk and asymmetric exclusion process.

already introduced in (2.1) and (3.3), gives the *typical scale* $n_c \simeq \frac{N}{\eta}$, above which we obtain straight aligned patterns. Here r_0 is a normalizing constant, which permits to fix the expected value $\bar{v}$ of the particle density

$$v = \frac{1}{N} \sum_{i=1}^{N} \mathbb{1}_{\{\alpha_i = 1\}},$$

that is

$$\bar{v} = \mathbb{E}(v) = \frac{1}{N} \sum_{i=1}^{N} q_i = \frac{1}{N} \sum_{i=1}^{N} \frac{r_i}{1+r_i}.$$

Letting $N \to \infty$, we analyze the limiting process under the *scaling*,

$$\eta \stackrel{\text{def}}{=} \lim_{N \to \infty} \frac{N\mu}{\lambda}, \tag{4.3}$$

where η, up to some abuse in the notation, is now a parameter independent of N. This is tantamount to assume that μ is implicitly a function of N.

Fixing $x = i/N$ and taking the expansion with respect to η/N in (4.2), we get the limit equation

$$r(x) = r_0 \exp(-2\eta x), \tag{4.4}$$

which implies in turn

$$\bar{v} = \int_0^1 dx \left(1 - \frac{1}{1+r_0 \exp(-2\eta x)}\right) = \frac{1}{2\eta} \log \frac{1+r_0}{1+r_0 \exp(-2\eta)}.$$

Consequently,

$$r_0 = \frac{\sinh(\eta \bar{v})}{\sinh \eta(1-\bar{v})} e^{\eta}.$$

The integral of the particle density, taken as a function of x, is shown in Fig. 10 and is given by

$$h(x) = \int_0^x du \left(1 - \frac{1}{1+r_0 \exp(-2\eta u)}\right) = \frac{1}{\eta} \log \left[\frac{1+r_0}{1+r_0 \exp(-2\eta x)}\right].$$

This asymmetric exclusion model can be solved under more general conditions, in particular with open boundaries, using matrix methods.[7] The above simple example confirms the observed fact that the correct scaling parameter is indeed η, and also somehow explains why the chain remains Brownian when $\eta \lesssim 1$.

4.1.2. The General Case at Steady State

Once the sequence $\{s^b\}$ is given, particles (a) form a simple exclusion process in an inhomogeneous environment, with transition rates at position i given by system (3.2).

Our basic claim rely on the reasoning carried out in Section 4.1.1 for a closed system, in which the number of particles is kept constant.

Letting $P(S^a, S^b)$ denote the invariant measure of the process $(S^a(t), S^b(t))$, we start from the elementary decomposition

$$P(S^a, S^b) = P(S^a \mid S^b)\, P(S^b) = P(S^b \mid S^a)\, P(S^a).$$

From the discussion in Section 3.2, we claim that the conditional probabilities $P(S^a \mid S^b)$ and $P(S^b \mid S^a)$ coincide with the equilibrium probabilities obtained in Eq. (4.1) *for each particle species*. This means exactly that, as long as there is no *current*, conditional detailed balance equations of type (4.1) still hold at steady state, just replacing $\lambda^{\pm}$ by $\lambda_a^{\pm}(i)$ and $\lambda_b^{\pm}(i)$.

Hence, letting

$$q_i^a = \mathsf{E}[s_i^a \mid S^b], \qquad q_i^b = \mathsf{E}[s_i^b \mid S^a]. \tag{4.5}$$

we can write, with regard to species (a),

$$\lambda_a^+(i)(1-q_i^a)\, q_{i+1}^a = \lambda_a^-(i)\, q_i^a(1-q_{i+1}^a), \qquad i = 1 \ldots N,$$

where sites $N+1$ and 1 are identified for periodic boundary conditions, and q_i^a [resp. q_i^b] is the random variable equal to the conditional probability of having one particle of type (a) [resp. (b)] in position i given the sequence $\{s^b\}$ [resp. $\{s^a\}$].

$$P(S^a \mid S^b) = \prod_{i=1}^{N} (s_i^a q_i^a + \bar{s}_i^a (1-q_i^a)), \tag{4.6}$$

where the q_i^a's depend implicitly of S^b.

A detailed proof of these assertions could be be readily obtained by a coupling argument. We simply quote that they are in fact a direct consequence of the form (3.1) of the generator G, together with the uniqueness of the forward Kolmogorov's equations applied to functionals of the Markov process $(S^a(t), S^b(t))$, which is irreducible and has a finite state space.

Introducing now the ratio

$$r_i^a \overset{\text{def}}{=} \frac{q_i^a}{1-q_i^a},$$

we obtain

$$\log[r^a_{i+1}] - \log[r^a_i] = \log\left(\frac{\lambda^-_a(i)}{\lambda^+_a(i)}\right). \tag{4.7}$$

By using (3.2), an easy algebra based on the boolean character of the s^b_i yields

$$\log\frac{\lambda^-_a(i)}{\lambda^+_a(i)} = (1-2s^b_i)\log\frac{\lambda-\mu}{\lambda+\mu} + (s^b_{i+1}-s^b_i)\log\frac{(\gamma-\delta)(\lambda+\mu)}{(\gamma+\delta)(\lambda-\mu)}, \tag{4.8}$$

with a similar equation for type b particles. In addition we observe that the constraints

$$r^a_{N+1} = r^a_1, \qquad r^b_{N+1} = r^b_1,$$

for periodic boundary conditions, will be automatically fulfilled as long as the system of particles (b) is globally neutral (i.e., particles and holes have the same cardinality), in which case

$$\sum_{i=1}^{N} (1-2s^b_i) = 0.$$

4.1.3. Explicit Form of the Invariant Measure when δ=0

When particule currents as well as any other type of unbalanced cycles (e.g., rotations of folded motifs with $\delta \neq 0$) are absent, one can expect the invariant measure to be written in a Gibbs form. From the preceding section, it is a simple matter to guess such an expression. Indeed, using (4.8), it is not difficult to check that the probability measure

$$P(S^a, S^b) = \frac{1}{Z}\exp\left[\beta \sum_{i<j} (s^a_i \bar{s}^b_j - s^b_i \bar{s}^a_j)\right], \tag{4.9}$$

with $\beta = \log\frac{\lambda-\mu}{\lambda+\mu}$, does satisfy the following detailed balance equations for (a) [resp. (b)] species,

$$\frac{P(\{\ldots(s^a_k=1),(s^a_{k+1}=0),\ldots\}, S^b)}{P(\{\ldots(s^a_k=0),(s^a_{k+1}=1),\ldots\}, S^b)} = \frac{\lambda^-_a(k)}{\lambda^+_a(k)} = \exp\left[(1-s^b_k-s^b_{k+1})\log\frac{\lambda-\mu}{\lambda+\mu}\right],$$

simultaneously, and also at the edges (i.e., $k=N$) owing to the neutrality conditions

$$\sum_{i=1}^{N} s^{a,b}_i - \bar{s}^{a,b}_i = 0,$$

corresponding to $N_a = N_b = N/2$ (Z is the normalizing constant). In the particule formulation, the symmetry arising from circular permutations between links (0, 1, 2, 3) writes

$$\begin{cases} s^a \to s^b, \\ s^b \to \bar{s}^a. \end{cases}$$

Up to some algebra, the above form (4.9) can be checked to statisfy this symmetry property, and is also the unique solution of $PG = 0$, where G is the generator defined in (3.1).

4.2. Closed Curves: Weak Convergence and Mean-Field-Like Limit for Large N

We will now combine the stationary product forms obtained for each particle species, according to the iterative scheme proposed at the end of Section 3.2. Throughout this section, the dependence on N of the random variables q_k^a, q_k^b, given by (4.5), is kept implicit for the sake of shortness in the notation.

In order to derive ergodic and central limit theorems, it will be useful to introduce $\{w_i^a, i \geqslant 0\}$ and $\{w_i^b, i \geqslant 0\}$, two families of independent and identically distributed Bernoulli random variables with parameter $1/2$ and taking values in the set $\{1, -1\}$. We assume that (S^a, S^b), $\{w_i^a, i \geqslant 0\}$, $\{w_i^b, i \geqslant 0\}$ are defined on the same probability space, without further comment.

Lemma 4.1. Let α_k, $k \geqslant 1$, denote a sequence of complex numbers satisfying the condition $\sup_k |\alpha_k| < \infty$.

There exists a probability space such that

$$\begin{cases} \dfrac{1}{N}\displaystyle\sum_{k=1}^{N} \alpha_k s_k^a = \dfrac{1}{N}\sum_{k=1}^{N} \alpha_k (q_k^a + \sigma_k^a w_k^a) + O(N^{-2}) \quad \text{a.s.}, \\ \dfrac{1}{N}\displaystyle\sum_{k=1}^{N} \alpha_k s_k^b = \dfrac{1}{N}\sum_{k=1}^{N} \alpha_k (q_k^b + \sigma_k^b w_k^b) + O(N^{-2}) \quad \text{a.s.}, \end{cases} \tag{4.10}$$

where

$$\sigma_k^a = \sqrt{q_k^a(1-q_k^a)}, \qquad \sigma_k^b = \sqrt{q_k^b(1-q_k^b)}, \quad \forall k \geqslant 1. \tag{4.11}$$

Proof. To analyze more precisely the coupling between the two families, remembering Eqs. (4.5) and (4.6), we introduce the Laplace transforms

$$\varphi_k^a(\alpha) \stackrel{\text{def}}{=} \mathsf{E}\left[\exp\left\{\frac{1}{N}\sum_{k=1}^{N}\alpha_k s_k^a\right\}\right] = \mathsf{E}\left[\prod_{k=1}^{N}[1+q_k^a(e^{\frac{\alpha_k}{N}}-1)]\right].$$

Then

$$\varphi_k^a(\alpha) = \mathsf{E}\left[\exp\left\{\frac{1}{N}\sum_{k=1}^{N}\alpha_k q_k^a + \frac{1}{2N^2}\sum_{k=1}^{N}\alpha_k^2 q_k^a(1-q_k^a) + O\left(\frac{1}{N^2}\right)\right\}\right].$$

On the other hand, starting from the equality

$$\mathsf{E}\left[\exp\left\{\frac{1}{N}\sum_{k=1}^{n}\alpha_k(q_i^a+\sigma_i^a w_i^a)\right\}\right] = \mathsf{E}\left[\exp\left\{\frac{1}{N}\sum_{k=1}^{N}\alpha_k q_k^a + \sum_{k=1}^{N}\log\cosh\frac{\sigma_k^a\alpha_k}{N}\right\}\right],$$

with regard to the (a) species, we observe that the value of σ_k^a given in (4.11) yields the matching

$$\mathsf{E}\left[\exp\left\{\frac{1}{N}\sum_{k=1}^{N}\alpha_k s_k^a\right\}\right] = \left[\mathsf{E}\exp\left\{\frac{1}{N}\sum_{k=1}^{N}\alpha_k(q_k^a+\sigma_k^a w_k^a) + O\left(\frac{1}{N^2}\right)\right\}\right]. \tag{4.12}$$

Since all random variables at stake are uniformly bounded, Eq. (4.12) yields at once (4.10), but only in distribution. To conclude the proof of the lemma, we make use of transfer and coupling theorems due to Skorohod and Dudley (see ref. 12, Thm. 4.30 and Cor. 6.11, 6.12), which allow to switch from equalities in distribution to almost sure properties, since on the original probability space the right member of system (4.10) is a measurable mapping of the left one. ▮

4.2.1. Fundamental Scaling, Thermodynamic Limit, and Fluctuations

For any i, $1 \leqslant i \leqslant N$, we put ad libitum $x = i/N$, $0 \leqslant x \leqslant 1$.

Proposition 4.2. Under the *fundamental scaling*

$$\begin{cases} \dfrac{\mu}{\lambda} = \dfrac{\eta}{N} + o\left(\dfrac{1}{N}\right), \\ \dfrac{\delta}{\gamma} = O\left(\dfrac{1}{N}\right), \end{cases}$$

the weak limits

$$\rho^a(x) = \lim_{N\to\infty} q^a_{xN} \qquad \text{and} \qquad \rho^b(x) = \lim_{N\to\infty} q^b_{xN} \tag{4.13}$$

exist and satisfy the autonomous system of deterministic nonlinear differential equations

$$\begin{cases} \dfrac{\partial \rho^a(x)}{\partial x} = 4\eta\rho^a(x)(1-\rho^a(x))\left(\rho^b(x)-\dfrac{1}{2}\right), \\ \dfrac{\partial \rho^b(x)}{\partial x} = -4\eta\rho^b(x)(1-\rho^b(x))\left(\rho^a(x)-\dfrac{1}{2}\right). \end{cases} \tag{4.14}$$

In addition, the assumed closure of the original random walk imposes the relations

$$\begin{cases} \int_0^1 \rho^a(x)\,dx = \int_0^1 \rho^b(x)\,dx = \frac{1}{2}, \\ \rho^a(x+1) = \rho^a(x), \\ \rho^b(x+1) = \rho^b(x). \end{cases} \tag{4.15}$$

Proof. Taking the expansion with respect to N in Eqs. (4.7) and (4.8), and using Lemma 4.1, we get after some algebra

$$\begin{cases} \log \dfrac{r^a_k}{r^a_1} = \dfrac{2\eta}{N}\displaystyle\sum_{j=1}^{k-1}(2q^b_j + 2\sigma^b_j w^b_j - 1) + O\left(\dfrac{1}{N}\right) \quad \text{a.s.}, \\ \log \dfrac{r^b_k}{r^b_1} = -\dfrac{2\eta}{N}\displaystyle\sum_{j=1}^{k-1}(2q^a_j + 2\sigma^a_j w^a_j - 1) + O\left(\dfrac{1}{N}\right) \quad \text{a.s.} \end{cases} \tag{4.16}$$

Since N is a parameter and x rather stands for a variable, it is convenient to introduce the following functions of x

$$q^a_N(x) \stackrel{\text{def}}{=} q^a_{[xN]}, \qquad r^a_N(x) \stackrel{\text{def}}{=} \frac{q^a_N(x)}{1-q^a_N(x)}, \qquad \sigma^a_N(x) \stackrel{\text{def}}{=} \sqrt{q^a_N(x)(1-q^a_N(x))},$$

and similarly for the (b) species.

To omit some tedious technicalities, we will only sketch the remaining lines of the proof.

First, it is not difficult to see that by restricting the expansion in (4.12) up to terms of order N^{-1}, and using the definition of r^a_k, r^b_k, we come to the simplified system

$$\begin{cases} q_k^a = \dfrac{r_1^a \exp\left[\dfrac{2\eta}{N}\displaystyle\sum_{j=1}^{k-1}(2q_j^b-1)\right]}{1+r_1^a \exp\left[\dfrac{2\eta}{N}\displaystyle\sum_{j=1}^{k-1}(2q_j^b-1)\right]} + O\left(\frac{1}{N}\right) \quad \text{a.s.}, \\ q_k^b = \dfrac{r_1^b \exp\left[-\dfrac{2\eta}{N}\displaystyle\sum_{j=1}^{k-1}(2q_j^a-1)\right]}{1+r_1^b \exp\left[-\dfrac{2\eta}{N}\displaystyle\sum_{j=1}^{k-1}(2q_j^a-1)\right]} + O\left(\frac{1}{N}\right) \quad \text{a.s.} \end{cases} \tag{4.17}$$

In a second step, it can be shown from (4.17), as in a purely deterministic context, that the quantities $q_N^a(x), q_N^b(x)$, form Cauchy sequences, hence converging, for all $0 \leqslant x \leqslant 1$. To see that the deterministic limits (4.13) exist and satisfy (4.14) is straightforward by approximating discrete sums by Riemann's integrals. This yields the differential system

$$\begin{cases} \dfrac{\partial}{\partial x}\left[\log\dfrac{\rho^a(x)}{1-\rho^a(x)}\right] = 2\eta(2\rho_b(x)-1), \\ \dfrac{\partial}{\partial x}\left[\log\dfrac{\rho^b(x)}{1-\rho^b(x)}\right] = -2\eta(2\rho_a(x)-1), \end{cases}$$

which has similarities with the famous Lotka–Volterra equations, where x plays here the role of the time. It is worth noting that (4.4) is immediately revisited, taking merely $\rho^b(x) \equiv 0$ (i.e., the density of particles (b) is kept constant). ▌

It is also tempting to get some insight into fluctuations around the above deterministic limit. This will be achieved by establishing the forthcoming central limit theorem.

Proposition 4.3. Under the *fundamental scaling*, the weak limits

$$g^a(x) = \lim_{N\to\infty} \sqrt{N}\,\frac{q_N^a(x)-\rho^a(x)}{\sigma_a^2(x)}, \qquad g^b(x) = \lim_{N\to\infty} \sqrt{N}\,\frac{q_N^b(x)-\rho^b(x)}{\sigma_b^2(x)}, \tag{4.18}$$

exist and satisfy the system of stochastic differential equations

$$\begin{cases} dg^a(x) = 4\eta[\sigma_a^2(x)\, g^b(x)\, dx + \sigma_b(x)\, dW^b(x)], \\ dg^b(x) = -4\eta[\sigma_b^2(x)\, g^a(x)\, dx + \sigma_a(x)\, dW^a(x)], \end{cases} \tag{4.19}$$

where

$$\sigma_a(x) \stackrel{\text{def}}{=} \sqrt{\rho^a(x)(1-\rho^a(x))}, \qquad \sigma_b(x) \stackrel{\text{def}}{=} \sqrt{\rho^b(x)(1-\rho^b(x))}.$$

Proof. Letting

$$X_N^a(x) \stackrel{\text{def}}{=} \frac{1}{\sqrt{N}} \sum_{k=1}^{[xN]} w_k^a, \qquad X_N^b(x) \stackrel{\text{def}}{=} \frac{1}{\sqrt{N}} \sum_{k=1}^{[xN]} w_k^b,$$

we consider the two white noise processes

$$W^a(x) \stackrel{\text{def}}{=} \lim_{N\to\infty} X_N^a(x), \qquad W^b(x) \stackrel{\text{def}}{=} \lim_{N\to\infty} X_N^b(x).$$

We call on a strong approximation theorem, which is a refinement of the invariance principle (see ref. 14: it shows how to construct $W^a(x)$ and $W^b(x)$ on the same probability space as X_N^a and X_N^b) in such a way that

$$\sup_{0\leqslant x\leqslant 1} |X_N(x) - W(x)| = O\left(\frac{\log N}{\sqrt{N}}\right).$$

Arguing as in the derivation of Proposition 4.2, we can write

$$\begin{cases} \log \dfrac{r_N^a(x)}{r_N^a(0)} = 2\eta \displaystyle\int_0^x du(2q_N^b(x)-1) + \frac{4\eta}{\sqrt{N}} \int_0^x \sigma_N^b(u)\, dW^b(u) + O\left(\frac{\log N}{N}\right), \\ \log \dfrac{r_N^b(x)}{r_N^b(0)} = -2\eta \displaystyle\int_0^x du(2q_N^a(x)-1) - \frac{4\eta}{\sqrt{N}} \int_0^x \sigma_N^a(u)\, dW^a(u) + O\left(\frac{\log N}{N}\right), \end{cases} \tag{4.20}$$

where the stochastic integrals are taken in the Itô sense (see ref. 15). Defining $g_N^a(x)$ and $g_N^b(x)$ by the equations

$$q_N^a(x) = \rho^a(x) + \sigma_a^2(x)\, g_N^a(x),$$
$$q_N^b(x) = \rho^b(x) + \sigma_b^2(x)\, g_N^b(x),$$

then putting these expressions into (4.20) and differentiating (4.20) (details are omitted), we are lead to 4.20. The proof of Proposition 4.3 is completed. ▌

Remark. Let us comment on the scaling of δ. Contrary to the scaling of μ, which is naturally dictated by homogeneity (the sums in (4.16) remain meaningful after dividing by N, when $N\to\infty$), it is a purely dynamical consideration which dictates the scaling of δ. Indeed, μ and δ

are associated with time constants τ_μ and τ_δ. The quantity τ_μ represents the typical unit of time for a free particle (a) or (b) to drift along the system over a finite distance, whereas τ_δ is a time-scale for rotations of vertical or horizontal fold $M2$ of the chain, remembering that δ stands for the *detuning* between γ^+ and γ^- defined in Section 1. Therefore either these time-scale are coherent and δ is rescaled, otherwise rotational motions of $M2$ occur at a shorter time scale and a different analysis has to be conducted, since motifs $M2$ (which correlate hole-particle pairs of species (a) and (b)) reach their equilibrium distribution before particles have enough time to move along the system. Numerically we could not perceive any specific effect related to δ, so that we restricted ourselves to the above *fundamental scaling*.

4.2.2. Second Order Phase Transition

Here we focus on on the deterministic (4.14) part of the equations. Using the notation

$$v_a(x) \stackrel{\text{def}}{=} 2\rho^a(x) - 1, \qquad v_b(x) \stackrel{\text{def}}{=} 2\rho^b(x) - 1,$$

apart from the trivial solution $v_a(x) = v_b(x) = 0$, we obtain from (4.14)

$$\frac{v_a(x)}{1 - v_a^2(x)} \frac{\partial v_a(x)}{\partial x} = -\frac{v_b(x)}{1 - v_b^2(x)} \frac{\partial v_b(x)}{\partial x},$$

or, after integration,

$$1 - v_a^2(x) = \frac{C}{1 - v_b^2(x)}, \qquad 0 < C < 1,$$

since $|v_a| < 1$ and $|v_b| < 1$. Plugging the last relation into (4.14) leads to

$$\left(\frac{\partial v_a(x)}{\partial x} \right)^2 = \eta^2 [1 - v_a^2(x)][1 - C - v_a^2(x)], \tag{4.21}$$

the solution of which is the standard Jacobi elliptic function

$$v_a(x) = \frac{1}{\sqrt{1 - C}} \operatorname{sn}(\eta x, \sqrt{1 - C}).$$

Finding the constant C is equivalent to compute the fundamental period of these functions. Hence, denoting by $X(C)$ the period of $v_a(x)$, we have to solve

$$X(C) = 1. \tag{4.22}$$

From (4.21) we see that $v_a(x)$ is bounded by $-\sqrt{1-C}$ and $\sqrt{1-C}$. Taking into account the constraint ($\int_0^1 v_a(x)\,dx = 0$), $X(C)$ is exactly given by

$$X(C) = \frac{1}{\eta} F\left(\frac{\pi}{2}, \sqrt{1-C}\right) = \frac{4}{\eta}\int_0^1 \frac{dv}{\sqrt{[1-v^2][1-(1-C)\,v^2]}},$$

where F is the standard elliptic integral of first kind.

$X(C)$ is a decreasing function of C on $]\,0, 1]$, reaching its minimum for $C = 1$, so that

$$X(C) \geqslant X(1) = \frac{2\pi}{\eta}.$$

Thus appears is a *critical value* for η, namely

$$\eta_c = 2\pi.$$

When $\eta_c < 2\pi$, (4.22) cannot be fulfilled and we are left with the trivial solution.

When $\eta_c \geqslant 2\pi$, it is straightforward to compute the arithmetic area $S_1(\eta)$ of the first winding sector, since it is indeed the only non-vanishing sector. Setting

$$\begin{cases} h_x(u) = \frac{1}{2}\int_0^u dv[v_a(v) + v_b(v)]\,dv, \\ \\ h_y(u) = \frac{1}{2}\int_0^u dv[v_a(v) - v_b(v)]\,dv, \end{cases}$$

$S_1(\eta)$ is simply the area enclosed by the curve $(h_x(u), h_y(u))\ u \in [0, 1]$, which is given by

$$S_1(\eta) = \frac{1}{2}\int_0^1 du\left[h_x \frac{\partial h_y}{\partial u} - h_y \frac{\partial h_x}{\partial u}\right],$$

or, after some algebra,

$$S_1(\eta) = \frac{1}{2\eta^2}\int_0^{\sqrt{1-C}} \frac{v}{\sqrt{(1-v^2)(1-C-v^2)}} \log\left[\frac{1+v}{1-v}\right] dv,$$

keeping in mind that C is also a function of η. The corresponding curve displayed in Fig. 5b matches pretty nicely all numerical observations, in particular with regard to the critical value η_c.

4.2.3. More about Fluctuations for $\eta < \eta_c$

When η is under the threshold η_c, the deterministic part becomes trivial, and we are left with fluctuations. This corresponds basically to the observations shown in Figs. 2a and 2b. Inserting

$$\rho^a(x) = \rho^b(x) = \tfrac{1}{2},$$

in (4.19), and setting

$$g(x) = g^a(x) + ig^b(x), \qquad W(x) = W^a(x) + iW^b(x), \tag{4.23}$$

we get solutions of the form

$$g(x) = -2i\eta \int_0^x e^{i\eta(u-x)}\, dW(u),$$

which corresponds to

$$\begin{aligned} q^a(x) = \frac{1}{2} + \frac{\eta}{\sqrt{N}} \Bigg[& \int_0^x (\sin(\eta(u-x))\, dW^a(u) \\ & + \cos(\eta(u-x))\, dW^b(u)) + dW^a(x) \Bigg] + o\left(\frac{1}{\sqrt{N}}\right), \\ q^b(x) = \frac{1}{2} + \frac{\eta}{\sqrt{N}} \Bigg[& \int_0^x (\cos(\eta(u-x))\, dW^a(u) \\ & - \sin(\eta(u-x))\, dW^b(u)) + dW^b(x) \Bigg] + o\left(\frac{1}{\sqrt{N}}\right). \end{aligned}$$

Hence we have derived an *equivalent* process, which up to order $o(\frac{1}{\sqrt{N}})$, describes the curves numerically observed. Letting

$$\begin{cases} h_N^a(x) \overset{\text{def}}{=} \dfrac{1}{N} \displaystyle\sum_{j=1}^{[xN]} (2s_j^a - 1), \\ h_N^b(x) \overset{\text{def}}{=} \dfrac{1}{N} \displaystyle\sum_{j=1}^{[xN]} (2s_j^b - 1), \end{cases}$$

the so-called equivalence says precisely

$$\begin{aligned} dh_N^a(x) &= h_N^a\left(x + \frac{1}{N}\right) - h_N^a(x) \\ &= 2q_N^a(x) + \frac{2}{\sqrt{N}} \sigma_N^a(x)\, dW^a(x) - 1 + o\left(\frac{1}{\sqrt{N}}\right) \end{aligned}$$

and the same holds for $dh_N^b(x)$. Introducing the complex function

$$h_N(x) = h_N^a(x) + ih_N^b(x),$$

we have

$$dh_N(x) = -\frac{2i\eta}{\sqrt{N}}\left[\int_0^x e^{i\eta(u-x)}dW(u) + dW(x)\right] + o\left(\frac{1}{\sqrt{N}}\right),$$

which, after integrating by parts, yields

$$h_N(x) = \frac{1}{\sqrt{N}}\left[\int_0^x 2e^{i\eta(u-x)}dW(u) - W(x)\right] + o\left(\frac{1}{\sqrt{N}}\right).$$

At this point it is possible to reconstruct the curves observed numerically, remembering that the discrete displacements (dx_i, dy_i) in the plane are expressed in terms of s_i^a and s_i^b as

$$\begin{cases} dx_i = 1 - s_i^a - s_i^b, \\ dy_i = s_i^a - s_i^b. \end{cases}$$

According to (4.23), we define

$$h(x) = \lim_{N\to\infty} \frac{1}{\sqrt{N}} \sum_{k=0}^{[xN]} (dx_k + i\,dy_k) \qquad \text{and} \qquad Z(x) = \frac{i-1}{2} W(x).$$

Then we have

$$h(x) = \int_0^x 2\exp[i\eta(u-x)]\, dZ(u) - Z(x).$$

This above equation accounts for the windings of the Brownian curve observed in Fig. 2b. When $\eta \to 0$, $h(x)$ coincides with the standard Brownian motion Z.

4.3. Burgers Equations in the Fluid Limit

In this section, without pretending to a detailed presentation, we propose a formal derivation of hydrodynamic equations describing the fluid limit of the particle density. They comprise the steady state solutions obtained in 4.2.

We start from the fact (which might be considered by the reader as an heuristic assumption) that the conditional independence of the s_i^a [resp. s_i^b], which is realized at time $t=0$ and at steady state, remains valid for all fixed time t, up to order $O(N^{-1})$. Exact proofs of this claim could be provided by adapting (up to sharp technicalities) some classical lines of argument proposed, e.g., in refs. 17, 9, and 22, together with a mean field type approach for the convergence of the semi-groups of the underlying Markov processes indexed by N.

Considering the stochastic variable which expresses the current of particles (a) between sites i and $i+1$ at time t, namely

$$\varphi_i^a(t) = \lambda_a^+(i,t)\, s_i^a(t)\, \bar{s}_{i+1}^a(t) - \lambda_a^-(i,t)\, s_{i+1}^a(t)\, \bar{s}_i^a(t),$$
$$\varphi_i^b(t) = \lambda_b^+(i,t)\, s_i^b(t)\, \bar{s}_{i+1}^b(t) - \lambda_b^-(i,t)\, s_{i+1}^b(t)\, \bar{s}_i^b(t),$$

we define the conditional expectation

$$J_i^a(t) = \mathsf{E}[\varphi_i^a(t) \mid S^b], \qquad J_i^b(t) = \mathsf{E}[\varphi_i^b(t) \mid S^a].$$

On account of the particle conservation principle, we have locally

$$\frac{\partial}{\partial t}\mathsf{E}[s_i^a(t)] + \mathsf{E}[\varphi_i^a(t) - \varphi_{i-1}^a(t)] = 0. \tag{4.24}$$

Then introducing the time dependent expectations $q_k^a(t)$ as functions of the sample path S^b

$$q_k^a(t) = \mathsf{E}[s_k^a(t) \mid S^b], \qquad q_k^b(t) = \mathsf{E}[s_k^b(t) \mid S^a], \tag{4.25}$$

we can write by (4.24)

$$\frac{1}{N}\sum_{k=1}^{N} \alpha_k (q_k^a(t) - q_k^a(0) + \int_0^t d\tau (J_k^a(t) - J_{k-1}^a(t))) = 0, \tag{4.26}$$

with again the condition $\sup_k |\alpha_k| < \infty$. Expressing the *almost* conditional independence of the s_k^a's, we have

$$\frac{1}{N}\sum_{k=1}^{N} \alpha_k \mathsf{E}_t[\lambda_a^+(k,t)\, q_k^a(t)(1-q_{k+1}^a(t)) - \lambda_a^-(k,t)\, q_{k+1}^a(t)(1-q_k^a(t))]$$
$$= \frac{1}{N}\sum_{k=1}^{N} \alpha_k J_k^a(t) + o\left(\frac{1}{N}\right).$$

To be consistent with the procedure developed for the stationary regime case, we substitute to the S^b the so-called equivalent set $\{q_k^b + \sigma_k^b w_k^b\}$ into the expressions of the rates given by

$$\log \lambda_a^{\pm}(i) = \log \lambda + 2(s_i^b + s_{i+1}^b - 2s_i^b s_{i+1}^b) \log \frac{\gamma}{\lambda}$$
$$\pm \frac{\eta}{N}(1 - s_i^b - s_{i+1}^b) \pm \frac{\delta}{\gamma}(s_i^b - s_{i+1}^b) + o\left(\frac{1}{N}\right),$$

according to the *fundamental scaling*. This insures that λ_a^+ and λ_a^- remain perfectly correlated. As for the the fluid limit, the procedure amounts simply to replace s_i^b by q_i^b in $\lambda_a^{\pm}(i)$, and to approximate all discrete sums in (4.26) by Riemann's integrals, for arbitrary $\alpha(x)$. This yields the continuity equation

$$\frac{\partial \rho^a(x, t)}{\partial t} = -\frac{\partial J^a(x, t)}{\partial x}, \tag{4.27}$$

where $\rho_a(x, t)$ and $J^a(x, t)$ are the deterministic continuous counterparts of $q_k^a(t)$ and $J_k^a(t)$. The current is now given by

$$J^a(x, t) = D\left[2\eta\rho^a(1-\rho^a)(1-2\rho^b) - \frac{\partial \rho^a(x, t)}{\partial x}\right] \exp\left(2\rho^b(1-\rho^b) \log \frac{\gamma}{\lambda}\right), \tag{4.28}$$

where we have introduced the diffusion constant

$$D \stackrel{\text{def}}{=} \lim_{N \to \infty} \frac{\lambda}{N^2},$$

λ being implicitly taken as a function of N. This scaling is confirmed numerically (see Fig. 5c). Actually we observe that the parameter γ controls the dynamics of the system through the definition of an effective diffusion constant. For particles (a), we have

$$D^a(x, t) \stackrel{\text{def}}{=} D \exp\left[2\rho^b(x, t)(1-\rho^b(x, t)) \log \frac{\gamma}{\lambda}\right].$$

with the corresponding relation for particles (b)). In the particular case $\gamma \to 0$, this constant vanishes, except at loci where the density of particles (b) has no fluctuations, that is $\sigma^2 = \rho^b(1-\rho^b) = 0$), in which case $D^a(x, t) = D$, as to be expected from the analysis of the stretched walk. When $\gamma = \lambda$, we obtain a dynamical system of deterministic equations

$$\frac{\partial \rho^a(x,t)}{\partial t} = D\frac{\partial^2 \rho^a(x,t)}{\partial x^2} - 2D\eta \frac{\partial}{\partial x}[\rho^a(1-\rho^a)(1-2\rho^b)](x,t),$$

$$\frac{\partial \rho^b(x,t)}{\partial t} = D\frac{\partial^2 \rho^b(x,t)}{\partial x^2} + 2D\eta \frac{\partial}{\partial x}[\rho^b(1-\rho^b)(1-2\rho^a)](x,t).$$

These equations belong to Burgers class. When taking one of the two density species (say (a)) to be a constant $\rho_a = 0$ or $\rho_a = 1$, the density of particles (b) is then driven by an ordinary Burgers equation describing the evolution of a stretched walk. For an arbitrary γ, the steady state solution of (4.27) is tantamount to let the current vanish in (4.28), which after integration gives system (4.14) independent of γ, as to be expected.

5. CONCLUSION AND PROSPECTS

The model of the discrete event system presented in this report turned out very friendly for simulation runs. Although the dimension be small (curves in the Euclidean plane), several basic phase-transition phenomena have been observed, among which a glassy phase. As we stove to point out, there are many ways to describe this system, which bring to light connections between various stochastic and algebraic formalisms.

Nonetheless, in our opinion, the most efficient way toward concrete mathematical and physical properties appears to be on the track of coupled exclusion processes. This mapping allows also to address the continuous limit considered in the last section, and this approach can be a method for coding numerical simulations. In this manner, we have been able to observe that when we alternatively freeze one of the subsystems, letting the other one reach its equilibrium, the whole process attains its stationary state, and moreover much quicker.

It is worth remarking the connection of our model with the so-called (ABC) model of ref. 10, which considers three particle species on a ring. In fact, if we map the sequences $(X_1,\ldots, X_N)$, $X_i \in \{A, B, C\}$, onto random walks on the triangular lattice. Then the letters A, B, C correspond to oriented links in the directions $0, \frac{2\pi}{3}, \frac{4\pi}{3}$, and the dynamics is obtained by exchanging left and right bends with rates 1 and q. Closed curves are obtained with a fair distribution of letters A, B, C. In this case, the authors can write an explicit form for the invariant measure, currents are absent, and the same kind of phase transition phenomenon appears. It is also worth mentionning, that a very similar although different model to ours, consisting of two coupled exclusion models has been introduced in the context colloidal sedimentation.[16]

In our model as far as dynamics is concerned, deeper investigations are needed in order to include fluctuations directly into the equations, and to clarify the role of the parameter δ. This would give a firm starting point to get an insight into slow dynamics and into the non-linear excitations which are swarming in the glassy phase (metastable states). Open boundary conditions and presence of currents would also be worth investigating. Actually, it seems possible to generalize the model to higher dimensions and to find related concrete applications, for example in biology (evolution of RNA and proteins). In particular in $\mathbb{R}^3$, we plan to adapt our model having in mind the existence of dynamical twistings.

ACKNOWLEDGMENTS

The authors want to thank Arnaud de La Fortelle (INRIA) and Kirone Mallick (CEA) for many valuable discussions. The second author also acknowledges Christophe Josserand (CNRS) for useful advices, especially about numerical experiments.

REFERENCES

1. C. L. Berthelsen, J. Glazier, and M. Skolnick, Global fractal dimension of human DNA sequences treated as pseudorandom walks, *Phys. Rev. A* **45**:8902–8913 (1992).
2. O. Bénichoux and J. Desbois, Windings of the 2d free rouse chain, *J. Phys. A. Math. Gen.* **33**:6655–6667 (2000).
3. J. Burgers, A mathematical model illustrating the theory of turbulences, *Adv. Appl. Mech.* **1**:171–199 (1948).
4. S. Cebrat and M. Dudek, The effect of DNA phase structure on DNA walks, *Eur. J. Phys.* **3**:271–276 (1998).
5. M. Clincy, B. Derrida, and M. Evans, *Phase Transition in the ABC Model*, cond/mat 0209674 (2002).
6. A. Comtet, J. Desbois, and S. Ouvry, Winding of planar brownian curves, *J. Phys. A: Math. Gen.* **23**:3563–3572 (1990).
7. B. Derrida, M. Evans, V. Hakim, and V. Pasquier, Exact solution for 1d asymmetric exclusion model using a matrix formulation, *J. Phys. A: Math. Gen.* **26**:1493–1517 (1993).
8. M. Doi and S. F. Edwards, *The Theory of Polymer Dynamics* (Oxford University Press, 1986).
9. R. Durrett, Ten lectures on particle system, in *Lecture Notes in Maths.*, Vol. 1608 (Springer, 1995), pp. 97–201.
10. M. Evans, D. P. Foster, C. Godrèche, and D. Mukamel, Spontaneous symmetry breaking in a one dimensional driven diffusive system, *Phys. Rev. Lett.* **74**:208–211 (1995).
11. P. D. Gennes, *Scaling Concepts in Polymer Physics* (Cornell University Press, Ithaca, NY, 1979).
12. O. Kallenberg, *Foundations of Modern Probability*, 2nd Ed. (Springer, 2001).
13. M. Kardar, G. Parisi, and Y. Zhang, Dynamic scaling of growing interfaces, *Phys. Rev. Lett.* **56**:889–892 (1986).
14. J. Komlos, G. Major, and P. Tusnady, An approximation of partial sums of independent rv's and the sample df i,ii., *Z. Warsch. verw. Gebiete* **32**:111–131 (1975, 1976).

15. B. Øksendal, *Stochastic Differential Equations* (Springer, 1985).
16. R. Lahiri, M. Barma, and S. Ramaswamy, Strong phase separation in a model of sedimenting lattices, *Phys. Rev. E* **61**:1648–1658 (2000).
17. T. M. Liggett, *Interacting Particle Systems*, Grundlehren der mathematischen Wissenschaften (Springer, 1985).
18. P. Lévy, *Processus stochastiques et mouvement Brownien* (Gauthier-Villars, 1948).
19. J. W. Pitman and M. Yor, Further asymptotic laws of planar brownian motion, *Ann. Probab.* **17**:965–1011 (1989).
20. P. Rouse, A theory of linear viscoelastic properties of dilute solutions of coiling polymers, *J. Chem. Phys.* **21**:1272–1280 (1953).
21. F. Spitzer, Some theorems concerning 2-dimensional brownian motion, *Trans. Amer. Math. Soc.* **87**:187–197 (1958).
22. H. Spohn, *Large Scale Dynamics of Interacting Particles* (Springer, 1991).